

Assessment of synergistic effects of LP-MOCVD TiO₂ and Ti surface finish on the performance of dental implants

Francesca Visentin^{*,a}, Alessandro Galenda^b, Monica Fabrizio^b, Simone Battiston^b, Nicola Brianese^b, Rosalba Gerbasi^b, Valentina Zin^b, and Naida El Habra^b

^aDepartment of Industrial Engineering, University of Padova, Via Gradenigo, 6/a, 35131 Padova, Italy

^bCNR-ICMATE Institute of Condensed Matter Chemistry and Technologies for Energy, Italian National Research Council, Corso Stati Uniti, 4, 35127 Padova, Italy

*Corresponding author francesca.visentin.7@studenti.unipd.it

KEYWORDS. Titanium dioxide, dental implants, corrosion resistance, wettability, MOCVD.

ABSTRACT: Three differently treated titanium substrates to be used in dental implant applications and with different surficial morphology were coated with 200 nm titanium dioxide (TiO₂) films by using Low Pressure Metal Organic Chemical Vapor Deposition (MOCVD) at 390°C and 100 Pa. No literature references were found on the performance evaluation of the TiO₂ MOCVD coatings on substrates with different pristine morphology; therefore in this work the influence of the pristine Ti surface characteristics on TiO₂ crystalline structure, morphology, wettability as well as on ion release, electrochemical behavior, tribocorrosion performance, and nano-mechanical properties were studied and discussed. In particular, it was shown that the pristine substrate influenced both the crystalline phases formation and crystallite size. Scanning electron microscopy analyses and roughness evaluation showed the optimal conformal coverage of all the MOCVD coatings for all substrates, with grain size depending on the substrate morphology and topography. The wettability of the TiO₂ coated Ti substrates highlighted a superhydrophilic behavior and, if stored in air, decreased as a function of the time ageing. Ions release tests, nanoindentation measurements, tribocorrosion, and potentiodynamic polarization experiments suggest.

INTRODUCTION

Nowadays, roughly 70%–80% of dental implants are manufactured from metallic biomaterials, such as stainless steels, cobalt–chromium alloys, and titanium and Ti alloys.[1] Among them, commercial pure titanium (cp-Ti) and its alloys have been widely used for dental implant applications due to their excellent combination of strength-to-weight ratio, corrosion resistance and biocompatibility.[2] An essential surface feature of Ti is its capability to form a thin (4–6 nm thick), stable, and amorphous TiO₂ layer under exposure to the atmosphere and/or physiological fluids. However, despite its excellent biocompatibility, native titanium dioxide rarely chemically bonds to bone tissue after implantation, consequently, Ti is often considered as an inert biomaterial.[3] Furthermore, although this passive layer is widely described as a protective interlayer, it is too thin and his chemical barrier action is not longtime effective under the action of body fluids. This makes the bulk material to undergo a slow but lasting metal ion release in the neighboring tissues,[4] especially at low pH and in the presence of fluoride (tooth paste for instance).[5] Metal ion release may activate body defense mechanisms and influence cellular activity, so adverse reactions and even implant rejections may take place.[4]

Starting from these considerations, in order to reduce unfavorable body reactions and, in the meantime, improve dental implants osseointegration, surface role becomes essential.[6] The relevance of changes in geometry, surface morphology and/or chemistry within the osseointegration process is extensively reported.[7,8] Concerning implant morphology, in the past, the most common machining technique for oral implants was turning. Nowadays, the market is dominated by implants with surface roughness higher than the turned component ones. Rougher surfaces are generally claimed to promote improved healing, thanks to their better mechanical anchorage to the bone. Many *in-vivo* and *in-vitro* studies have shown a better osseointegrative response of rougher surfaces when compared to smoother ones,[9] and the significance of nanostructured surfaces has been documented.[9] In the work of Kubo et al.[10] it is shown that TiO₂ nanonodules onto micro-pitted acid-etched Ti surfaces enhanced the attachment, spread, proliferation, and differentiation of osteoblasts. Moreover, Cochran et al.[11] compared micro/nano-porous implants (i.e. sandblasted and acid-etched, SLA) with microporous implants (i.e. titanium plasma spray, TPS) and found higher bone-to-implant contact for the rougher surfaces (SLA implants). However, rougher surfaces may have clinical drawbacks, such as marginal bone resorption and/or increased ion release.[12] Simultaneously to the increase of the implant roughness, various surface treatments have been

applied in order to modify the surface chemistry, developing targeted layers with improved functional characteristics for achieving faster and durable biological responses.[13] In this field, coatings based on titanium dioxide (TiO₂) are especially important for Ti surface modification, due to their good osseointegration properties, high corrosion resistance, and thermal stability.[14] Several *in-vitro* and *in-vivo* studies evidenced the positive effect of the functionalization of Ti surface with titania layer: rutile and anatase layers, compared to native TiO₂, demonstrate enhanced bioactivity in simulated body fluids.[15,16]

Low Pressure Metal Organic Chemical Vapor Deposition (LP-MOCVD) is a widely used technique for depositing crystalline TiO₂ thin films at relatively low temperature. Moreover, it is particularly suitable on complex-shaped samples, such as dental implants.[17] MOCVD technique has been already successfully applied to titanium dioxide deposition on dental implants, as demonstrated by several biological tests both *in-vitro* and *in-vivo*. [15] Specifically, Baryshnikova et al.[18] showed that nanostructured TiO₂ growth via MOCVD technique may act as a bioactive material inducing formation on its surface of hydroxyapatite (HA), Ca₁₀(PO₄)₆(OH)₂, the basic inorganic component of bone tissue. Moreover, besides the intrinsic bioactivity of the crystalline titania thin films, TiO₂ layer on Ti substrate may also be used as a glue-layer for the subsequent deposition of the highly bioactive Calcium Phosphate Ceramics (CPCs).[19,20] Lastly, crystalline TiO₂ layers may have an influence on the photoactivity of the Ti implant surface. Indeed, such titania functionalized surfaces would be sterilized simply with the use of UV illumination. In this way, the same coating could perform two tasks: enhance the osseointegration process and contribute to the surface disinfection process.[14]

Surface morphology and topography of the Ti surface significantly affect the rate and quality of osseointegration and, to our knowledge, the exact role of surface chemistry and texture on the early stages of the osseointegration remains poorly understood.[21] In this work, with the aim of improving the titanium surface properties, LP-MOCVD technique was employed in order to deposit conformal crystalline TiO₂ on Ti substrates. The purpose of this study was to investigate the influence of the pristine titanium morphology and topography on crystalline structure, morphology and surface wettability of TiO₂ coatings. Ion release tests, electrochemical and tribocorrosion experiments, and nanoindentation measurements were also carried out.

EXPERIMENTAL SECTION

Materials

Medical grade IV Ti was kindly provided by RT srl (Albignasego, Padova, Italy). Since the geometrical shape of dental implants is often not directly analyzable by the laboratory-scale characterization techniques, most of the studies were carried out on flat substrates that accurately reproduce the surface features of typical implants.

Titanium (IV) tetraisopropoxide (TTIP) 97% from Sigma-Aldrich was used as titanium precursor. Lactic acid (LA) 90% and phosphate-buffered saline (PBS) were purchase from Labochimica srl and Sigma Aldrich, respectively. The chemical composition for the artificial saliva was KCl (0.4 g/L), NaCl (0.4 g/L), CaCl₂·2H₂O (0.906 g/L), NaH₂PO₄·2H₂O (0.690 g/L), Na₂S·9H₂O (0.005 g/L), and urea (1.0 g/L).[13] All the reagents were purchase from Sigma Aldrich. HCl 37% from Sigma Aldrich and H₂SO₄ 96-98% from Carlo Erba were employed for the etching of the substrates. All the chemicals were used as received without any further purification.

Employed water was always freshly deionized and Simplicity (Millipore) system was used to prepare ultrapure water (18.2 MΩ/cm).

Preparation of the surfaces and film deposition

Three types of surfaces (i.e. Ti machined, sandblasted, and sandblasted/acid etched) were used as titanium substrates, all commercial grade IV. Ti discs (φ = 8 mm) or implants (cylindrical implants with truncated cone end, external hexagon geometry, height: 10 mm; φ = 4 mm) were treated according to the following three different surface modification procedures, in order to obtain various surface characteristics:

- (a) Machined (m) samples, named “Ti m”, were used as received from RT srl;
- (b) Sandblasted (s) samples, named “Ti s”, were sandblasted by RT srl with Al₂O₃ particles;
- (c) Sandblasted/acid etched (s+a) samples, named “Ti s+a”, were initially sandblasted (following the same procedure of samples (b)) and then treated with an acid solution (HCl and H₂SO₄ solution according to an internal procedure) at 80°C for 30 min.

For all the Ti substrates, a final cleaning process, with soap and ultrasound, was finally applied.

TiO₂ deposition on titanium substrates was carried out by using a custom-made hot wall MOCVD reactor, obtaining sample named Ti_m-TiO₂, Ti_s-TiO₂, and Ti_{s+a}-TiO₂, respectively. Depositions were carried out at a reactor pressure of 100 Pa and at the temperature of 390°C. TTIP (kept at 40°C, carried into the reactor by a 110 sccm N₂ flow) was used as the metal organic precursor. No co-reagents were used. The TiO₂ thickness was about 200 nm, in accordance with literature references,[20] in order to obtain the best compromise between the increase of the Ti corrosion resistance and the opti-

mal coating/substrate adhesion features, preserving the pristine substrates roughness.[22] The synthesis procedure and composite material are patent pending.[23]

Characterizations

The surface morphology of the samples was investigated by Sigma Zeiss field emission scanning electron microscope (FE-SEM) with an electron beam acceleration voltage of 5 kV. Prior to the analyses, the samples were coated with 15 nm of Pt by Emitech K575X Turbo Sputter Coater. Energy dispersive X-ray spectroscopy (EDS) qualitative analyses were obtained with an Oxford X-Max system at an accelerating voltage of 15 keV.

Thin film thickness was evaluated from spectral reflectance measurements by using a Filmetrics F20 thin film analyzer, operating in the 200-1100 wavelength range.

3D maps and roughness parameters (Ra, Rq, Rz, Rp, Rv, Rt) were calculated before and after the MOCVD coating processes using a stylus Profilometer Bruker Dektat XT, according to ISO 3274:1996 and ISO 4288:1996. For each sample type, five different samples were investigated, each of them by five measurements profiles with a respective scan length of 4.8 mm, with a cut-off Gaussian digital filter length of 0.8 mm separating roughness from waviness, and with a measurement speed of 50 $\mu\text{m/s}$. The surface area excess compared to smooth Ti was also calculated (Sdr value, developed interfacial area ratio). It is expressed as the ratio between the real surface area and the geometrical area.

The crystallographic structure was determined by X-ray diffraction (XRD) performed by means of a Philips X'Pert PW 3710 powder diffractometer operating in Bragg-Brentano θ - 2θ geometry mode, using Cu K α radiation ($\lambda = 0.154$ nm, 40 kV and 30 mA). Phase identification was performed with the support of the standard 2002 ICDD database files. The relative phase amount and the crystallite sizes were estimated by Rietveld refinement by means of the MAUD (Material Analysis Using Diffraction) software[24] and using COD structures.

Static contact angles were measured by the sessile drop technique. A drop of 10 μl deionized water was deposited on the surface of the sample and observed by a CCD camera. Tests were carried out in ambient laboratory temperature range 20-25°C and at constant relative humidity (RH~ 43% \pm 5%). The equilibrium contact angles were measured after 20 seconds from water drop depositions. ImageJ software (plugin LB-ADSA) was used in order to evaluate the contact angle values. The reported values are the average of at least 5 determinations.

In-vitro titanium and aluminum ion release was evaluated by means of inductively coupled plasma atomic emission spectroscopy (ICP-AES), performed by Thermo Scientific iCAP 6000 DUO, equipped with: a CID (Charge Injection Device) solid-state detector, which allows the simultaneous reading of wavelengths in the range of 166-847 nm; a DUAL VIEW device (axial view + radial view); an RF generator with software-controlled power-adjustable at 4 values: 750, 950, 1150, 1350 W. Calibration solutions were prepared from Carlo Erba mono-elemental standard solutions (1000 $\mu\text{g/ml}$). Five solutions with concentrations of 0, 1, 3, 6 e 10 $\mu\text{g/ml}$ (ppm) for each element were used for calibration curves. For these experiments, cylindrical implants with truncated cone end with ϕ : 4 mm, length: 10 mm; weight: 372 \pm 10 mg were used. Three of each type of specimen (Ti m, Ti s, Ti s+a; Ti m_TiO₂, Ti s_TiO₂, Ti s+a_TiO₂) were separately immersed in 10 mL of 1% lactic acid aqueous solution (pH=2.4) or in 10 mL of 0.1mol/L phosphate-buffered saline solution (pH=7.4). The former was used as a more aggressive medium, while the second in order to simulate biological environmental pH. Each specimen was placed in its individual plastic bottle with a cap. The entire specimen was completely submerged in the release test solution, kept at 37°C and shaken in a reciprocating shaker for 28 days at 60 cycles/min. After 28 days of immersion, the ion concentrations released from the specimens into each solution was analyzed. The amount of released ions (Ti and Al) was calculated as micrograms per implant. The mean quantity and standard deviation were calculated and compared with blank experiments.

Tribocorrosion characterization was carried out with a Bruker UMT-2 tribotester set for pure sliding and operating in ball-on-flat configuration and linear reciprocating motion mode, equipped with a standard three-electrode electrochemical cell. The titanium samples were used as the working electrode, a platinum wire was the counter electrode and the reference electrode was Ag/AgCl (KCl 1M, -10 mV vs SCE). The reciprocating sliding tests were performed against an alumina ball (ϕ 5mm) at an initial Hertzian contact pressure of 400 MPa, sliding speed of 6 mm/s, sliding distance of 3 mm, in order to realize a frequency of 1 Hz. The biological environment was simulated by artificial saliva (AS), which was maintained at 37°C during the whole duration of the tests. The pH of the electrolytic solution was stabilized around 6 at T = 37°C. Tribocorrosion behavior was investigated by means of open-circuit potential (OCP) measurements and sliding tests with potential recording as a function of sliding period. The test sequence was mainly constituted of three stages: (1) initial stabilization period; (2) sliding period; and (3) final stabilization period. During the sliding process, coefficient of friction (COF), lateral and vertical force were simultaneously recorded.

Throughout the potentiodynamic polarization experiments, the working electrode was polarized from -2.5 V to 7.5 V vs SCE at a scanning rate of 2 mV/s, in artificial saliva at 37°C. The exposed surface was ϕ 1.4 cm circular zone, for an overall area of 1.54 cm². J_0 was calculated considering also the mean roughness of the samples, by exploiting the Sdr (developed interfacial area ratio) parameter obtained from three-dimensional profilometry results. Thus, the actual exposed area was estimated for each surface finishing, taking into account the contribution of surface roughness. Finally, Tafel plots have been derived.

The nanoindentation test is a way to estimate the mechanical properties of a material at the nano-scale. A force (P) is applied to the surface to be indented by means of a diamond tip with known geometry while the values of the penetration depths (h) are continuously recorded as a function of P. Nanomechanical properties were evaluated by nano-indentation tests (NanoTest, Micro Materials Ltd) using a Berkovich pyramid-shaped diamond tip and operating in the depth control mode (30 s loading / 5 s load holding / 30 s unloading, thermal drift measurement 30 s). The maximum depth reached after loading phase was 30 nm in order to minimize the influence of the underlying substrate.[25] The thermal drift and compliance were automatically corrected by the software. The hardness (H) and the Elastic modulus (E) were evaluated using the method of Oliver and Pharr;[26] the results correspond to an average of a minimum of 45 indents.

All quantitative data are reported as the mean \pm standard deviation. For the assessment of the differences between groups, the analysis of variance (One-Way ANOVA) was applied and statistical differences between the samples were determined by Tukey's multiple comparison. A p-value <0.05 was taken to indicate statistical significance.

RESULTS AND DISCUSSION

As soon as a dental implant is placed into the bone, the body tissue interacts with its outermost layer.[17] Thus, when a Ti dental implant is inserted into the human jawbone, the adjacent tissues come into direct contact with the few nanometers-thick TiO₂ native layer, which is not enough passivating, crystalline and homogeneous.[17] In order to assess the features of TiO₂ coatings deposited on different Ti substrates 200 nm of titanium dioxide films were deposited by LP-MOCVD on machined, sandblasted, and sandblasted/acid etched Ti substrates (commercial grade IV) and extensively characterized.

1. Morphological characterization

Surface morphology has a noticeable effect on cell adhesion, extension and sequence.[9] Scanning Electron Microscopy (SEM) analyses showed the pristine morphology of machined (Figure 1a, 1b) sandblasted (Figure 1c, 1d) and sandblasted/acid etched (Figure 1e, 1f) surfaces. Machined substrates (Figure 1a, 1b) had the surface morphology of as-received machined implants, without any treatment (except the washing procedure, of course). The turning process generated tool marks and the surface was clearly anisotropic with directional irregularities. In Figure 1c and 1d, it can be observed that the alumina sandblasting process clearly modified the implant surface morphology and a homogeneous and isotropic surface structure was evident. Alumina is a commonly used blasting material, yielding a surface roughness that depends on the size of the blasting media.[7] Unfortunately, alumina residues often remain after the cleaning procedures (alumina is insoluble in acid, so it is particularly hard to remove), thus blasting material is frequently embedded into the implant surface. These residues must be particularly taken into account, because they could be released into the surrounding tissues (therefore negatively interfering with the osseointegration process) or create chemical heterogeneity that decrease the titanium corrosion resistance.[7] EDS analyses confirm the presence of alumina residues (generally about 11 wt. %). The surface morphology of sandblasted/acid etched samples (Figure 1e, 1f) is appears more isotropic than the turned and sandblasted surface ones. The sandblasting process and the following acid treatment changed the implant surface morphology: multi-level pores (induced from alumina sandblasting and acid etched processes) can be detected. The high magnification image (Figure 1f) shows nanometric grooves resulting from etching procedure. EDS analysis revealed that the acid etching process allowed the whole removal of sandblasting particles, as confirmed also by XRD characterization, presented later.

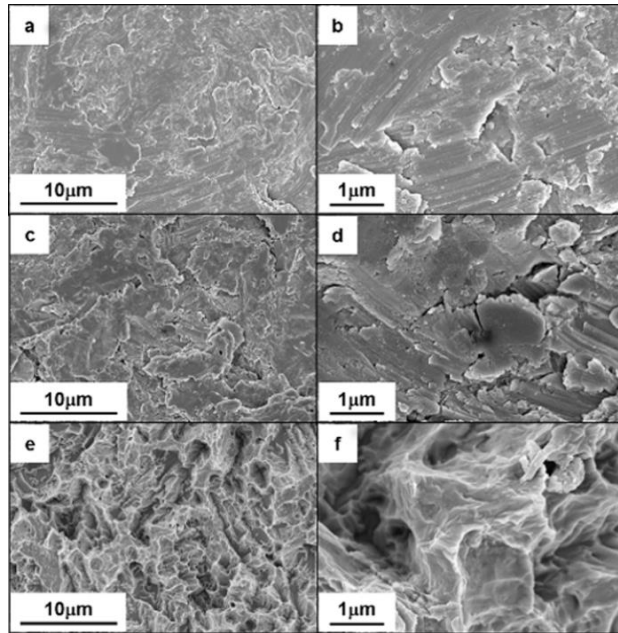


Figure 1. Secondary electron SEM images of Ti substrates before the MOCVD TiO_2 deposition: machined surfaces (a, b); Al_2O_3 sandblasted surfaces (c, d); sandblasted/acid etched surfaces (e, f).

Figure 2 shows SEM images of the Ti substrates after the LP-MOCVD process. It can be observed that the MOCVD films were conformal, even though the pristine substrate surface was rough, and the TiO_2 film matched the profile of the substrate below.[22] The typical titania morphology, with an angular platelet-like structure, was detectable at high magnification. Precisely, in Ti sandblasted coated samples ($\text{Ti}_s\text{-TiO}_2$) and in Ti sandblasted/acid etched coated samples ($\text{Ti}_{s+a}\text{-TiO}_2$) the grains appeared slightly less sharp and smaller than that of Ti machined coated ones ($\text{Ti}_m\text{-TiO}_2$).

Because of the ductile nature of the titanium substrate (i.e. not easily sectionable), in order to analyze the coatings along the sections, titania layers were deposited on Si (100) substrates. From cross sections of SEM images of a titania layers deposited on Si under the same experimental conditions of titanium substrates, a 200 nm titania layer with a compact structure can be obtained with a growth rate of 25 nm/min. This is consistent with previous studies where it was shown that under similar growth conditions, the deposited titania assumed a compact structure as long as the thickness is less than 400 nm, and a columnar structure formed upon increasing the thickness.[17,27] Spectral reflectance thickness evaluations of titania films on titanium machined substrates, confirmed the results.

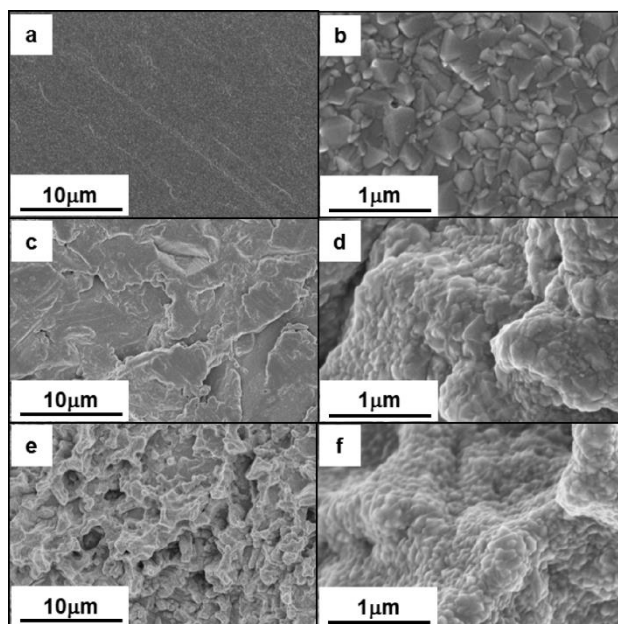


Figure 2. Secondary electron SEM images of the pristine Ti substrates after the MOCVD TiO₂ deposition: machined surfaces (a, b); Al₂O₃ sandblasted surfaces (c, d); sandblasted and acid etched surfaces (e, f).

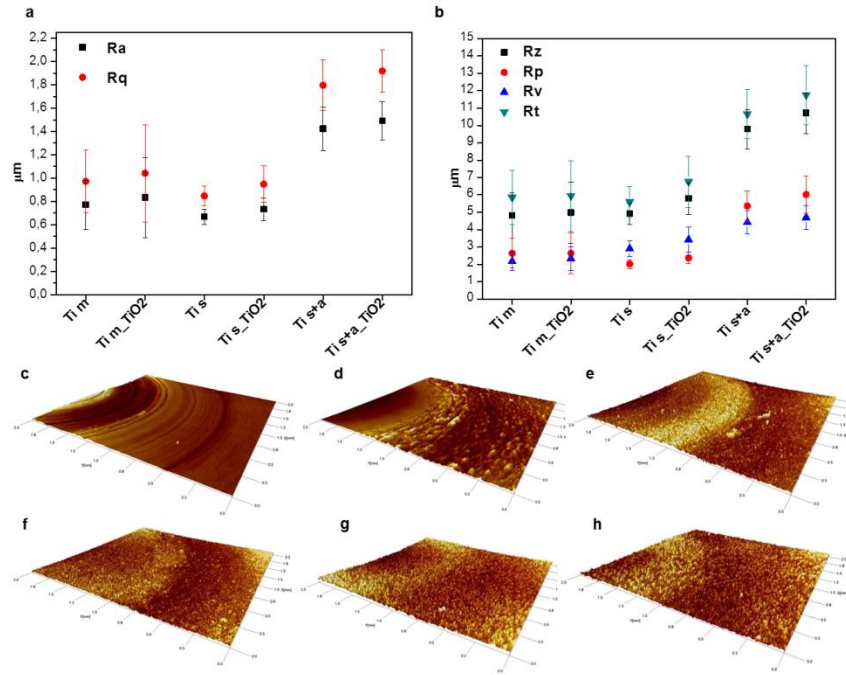


Figure 3. Roughness parameters (a, b) and $2\mu\text{m} \times 2\mu\text{m}$ 3D maps (c-h) for Ti substrates (Ti m, Ti s, Ti s+a) and for the corresponding MOCVD coated surfaces (Ti m_TiO₂, Ti s_TiO₂, Ti s+a_TiO₂).

3D maps and roughness parameters (Figure 3) were estimated using a stylus profilometer. From the investigation of the roughness parameters, it can be seen that both “m” and “s” surfaces, uncoated and coated, had similar roughness parameters, but sandblasted ones appeared more homogeneous. For Ti m and Ti s uncoated surfaces, Ra (arithmetic average roughness) values were not significantly different, at a 0.05 level, but the mean Ra value for Ti s+a substrates was higher. Moreover, “s” surfaces had valleys that were more pronounced than the peaks ($R_v > R_p$), conversely for “s+a” ones. R_t values were almost equal to R_z ones, indicating that the different samples investigated in the scan length were quite homogeneous. The roughness evaluations also confirmed the optimal MOCVD conformal coverage, already detected from SEM analyses: the roughness parameters, for each typology of surface, before and after the MOCVD process, were almost the same. Indeed, even if from Figure 3a slight increase of the Ra values of the coated samples could be observed (7% for Ti m_TiO₂, 8% for Ti s_TiO₂ and 5% for Ti s+a_TiO₂), it was restrained and the data analysis did not show any difference between the means value at a 0.05 significance level. In accordance with Popescu et al.[22] thin titania coatings (thinner than 1 micron) did not strongly influence the intrinsic substrates roughness and only long deposition times (i.e. thicker film) favored the formation of big crystal clusters that led to increase the roughness. For dental implant applications, it is important to calculate the effective surface area of the surface because this parameter is expected to influence the total amount of surface absorbed proteins Surface area excess (Sdr) compared to smooth Ti surface was also calculated (Ti m: 0.01, Ti s: 0.33, Ti s+a: 0.45). As expected, the highest surface area values were found in the “s+a” samples, while the lowest ones in the “m” samples. Comparing the roughness parameters and the Sdr values, it seems that machined surfaces had grooves, which increased the roughness parameters but not the effective surface area.

2. Structural characterization

X Ray Diffraction (XRD) analyses were carried out on Ti substrates (Figure 4a) and after the coating depositions (Figure 4b). All the Ti substrates were composed of hexagonal Ti (ICDD: 01-089-5009). Moreover, Ti m and Ti s+a substrates showed preferential orientation mainly with respect to (002) and (100) planes, correspondingly. Specifically, machined substrate were (002) oriented: this feature could be attributed to a superficial mechanical stress induced by the turning process. Indeed, no preferential orientation was detected in the Ti s sample, likely suggesting that the preferential orien-

tation was just located only on the Ti m surface. Differently, s+a substrate could be (100) preferential orientated because this face orientation was chemically more stable and consequently less etched during the chemical subtractive procedure.

Rietveld refinement of XRD patterns confirms previous EDS observations: Al₂O₃ residues from sandblasting process (about 13 wt. %) were detected on “s” substrates, while acid etching process allowed the whole removal of sandblasting particles. In the Ti s+a substrate titanium hydride was also found after the etching, as reported in literature.[28] After MOCVD process, crystalline TiO₂ in anatase (ICDD: 01-084-1286) phase was detected in all the substrates, without preferred orientation. The anatase mean crystallite size was dependent on the substrate typology: about 104 nm for Ti m-TiO₂, while Ti s and Ti s+a showed similar values: about 48 and 50 nm, respectively. Ti s-TiO₂ sample also showed TiO₂ in rutile phase (ICDD: 01-088-1172), 25 wt. % calculated from Rietveld refinement. In this field, it could be supposed that alumina residues can catalyze the rutile formation. Furthermore, XRD analysis shows that the MOCVD temperature (390°C) induced the whole decomposition of TiH₂, in accordance with literature references.[29]

3. Functional characterization

3.1. Wettability and storage conditions

Taking into account that osseointegration is favored at high implant surface availability, surface wettability is another parameter has to be carefully evaluated.[28] In literature, it is described that hydrophilicity presents major benefits during the initial stages of wound healing and during the subsequent osseointegrative events, facilitating bone integration.[30] Zhao et al.[31] showed that osteoblasts cultivated in hydrophilic and chemically pure surfaces had higher levels of differentiation markers than those cultured in hydrophobic surfaces. Furthermore, *in-vivo*[30] and clinical studies[32] showed that hydrophilic surfaces improve the bone-to-implant contact (BIC) and the bone anchorage during the early stages of bone healing. Surface wettability is affected by numerous factors; among them it is worth to mention topography, roughness, and chemical composition. Many investigations analyzed the influence of surface roughness on wettability and the conclusion is that roughness increases the water contact angle if its value on the un-roughened surface of the same material is higher than 90° and decreases it if the contact angle is lower than 90° (i.e. roughness makes hydrophilic surfaces more hydrophilic, hydrophobic ones more hydrophobic).[33] Acid etched surfaces are generally described to be hydrophobic.[28] Another factor affecting the surface wettability is the contamination of the surface: a decrease in wettability has been reported due to the increasing contamination of the surface by atmospheric hydrocarbons.[28]

Static water contact angles (CA) measurements are showed in Figure 5. Uncoated Ti substrates have characteristic wettability: 83° for Ti m, 79° for Ti s and 133° for Ti s+a. A possible explanation for the higher hydrophobicity of Ti s+a samples is in the topography generated by the acid attack. After TiO₂ deposition, the contact angle of water droplet plummeted to zero, suggesting a superhydrophilic behavior for all the samples. However, TiO₂-coated samples stored in air, were easily contaminated due to organic contamination[28] and the wettability slowly decreased (in laboratory air environment, recontamination of high-energy surfaces is unavoidable). As organic molecules are progressively absorbed, the initially hydrophilic behavior gradually turned into hydrophobic or less hydrophilic. This process modify the surface composition and surface reactivity, affecting firstly the protein absorption, subsequently the cell attachment, proliferation, differentiation and finally the osseointegration process.[30,34] Furthermore, it can be observed that the initial (first hours) loss of superhydrophilic features was faster for the ‘m’ and ‘s’ coated samples in comparison with the ‘s+a’ coated ones. This is likely due to the higher effective surface area of the ‘s+a’ coated samples (higher Sdr): greater surface area means larger number of attached -OH groups and, consequently, more hydrophobic molecules are needed in order to cut down the hydrophilic behavior. However, after about 20 days, the surface wettability of the MOCVD coated samples becomes comparable with that of the corresponding uncoated ones.

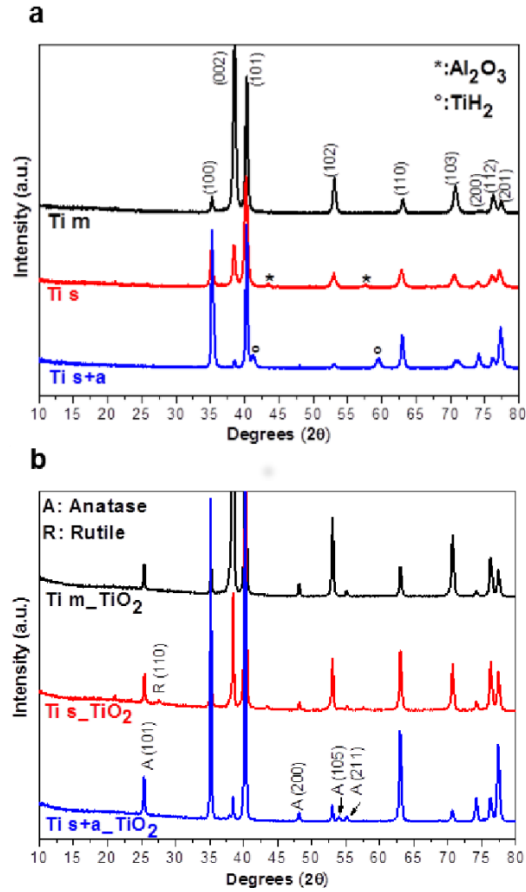


Figure 4. XRD patterns of uncoated Ti substrates (a) and MOCVD TiO_2 coated Ti substrates (b).

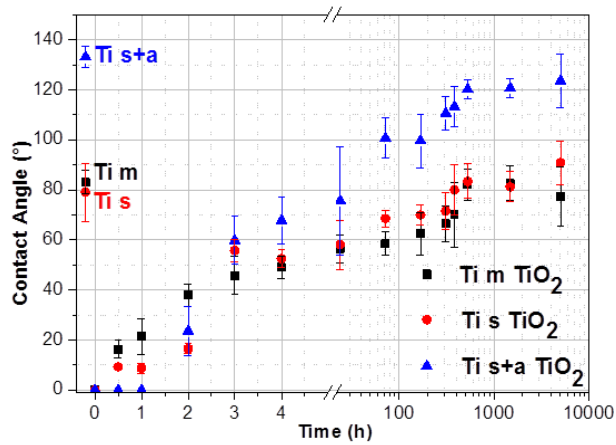


Figure 5. Contact angle before, just after the TiO_2 MOCVD process (time 0) and as function of time ageing for machined (Ti m), sandblasted (Ti s) and sandblasted/acid etched (Ti s+a) substrates.

Nowadays, implant shelf life is principally related to the maintenance of their sterility. Conversely, other components (i.e. hydrocarbons or C- and O- species from air pollution) could progressively adsorb on the titanium surface. Theoretically, an implant surface is perfectly clean only if it uniquely consists of Ti and O with chemical bonds between them, [34] but other elements were often identified in all the commercial implants. [34] As a consequence of organic surface contamination, implant failure could also be due to an inappropriate implant surface composition. [34] It follows that it is crucial to control the steps between implant surface functionalization and surgical application. Storage, being the last step before

application, directly influences the *in-vivo* performance of implants. Taking into account these considerations, different approaches could be followed in order to have durable clean hydrophilic surfaces while, in the meantime, maintaining the topography, the roughness and the crystalline structure of the pristine substrates.

In this work, in order to have durable (over long period, comparable with sterility shelf life) superhydrophilic surfaces two industrial-scalable strategies were taken into account. The first approach is the isolation of the clean titania superhydrophilic surface by preservation under liquid media.[9,34–37] Indeed, in theory, it could be possible avoid atmospheric poisoning by storing the sample in deionized water, in order to protect the surface from hydrocarbon contamination.[9,37] For this purpose, the just coated titania MOCVD samples (i.e. as freshly prepared titania coated Ti surfaces) were stored in plastic bowls filled with Milli-Q water. Milli-Q water was used as the simplest aqueous medium and in order to avoid the influence of other inorganic ions.[35,36] The experiments (Figure 6a), carried out for six months, have shown that this approach permits high hydrophilicity ($CA < 20^\circ$) and the slight wettability worsening is most likely due to the hydrocarbon contamination of the storage solution with time. Finally, it may be underlined that the roughest surfaces present longer superhydrophilic behavior. Indeed, as can be seen in Figure 6a, Ti s+a TiO_2 maintained high wettability also after 10 months. As it was previously observed (Figure 5), ‘s+a’ coated samples have reduced loss of superhydrophilic behavior, when compared with smoother surfaces. It is worth underlining that the slight oscillations of the low contact angle values ($CA < 15^\circ$) are ascribable to the intrinsic instrumental uncertainty.

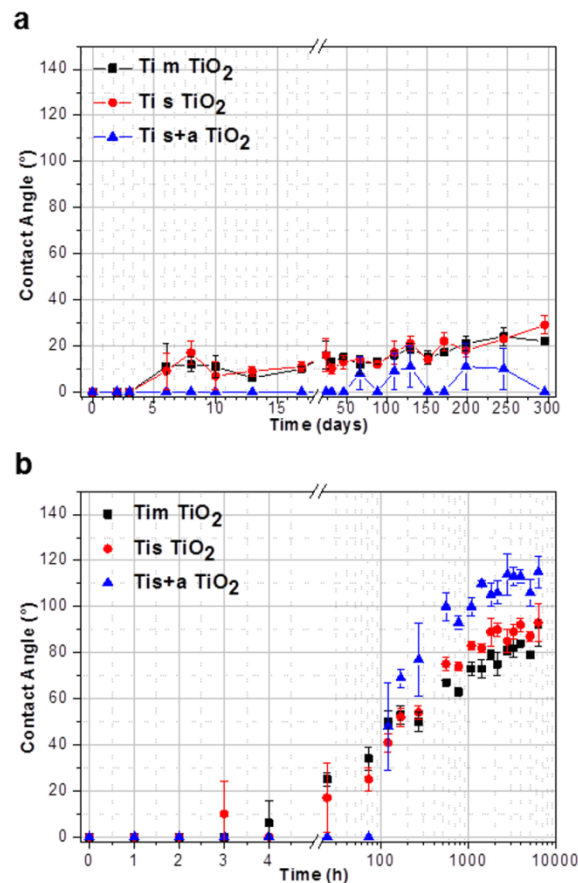


Figure 6. Evolution of the contact angle with aging time for the titania coated Ti substrates stored in Milli-Q water (a). Re-establishment of the TiO_2 superhydrophilicity by UV treatment and evolution of the contact angle with aging time for the titania coated Ti substrates stored in air (b).

Previous studies,[9,34–37] performed in water or in saline solution, on titanium substrates or titania functionalized Ti surfaces, were always carried out for shorter ageing time, not comparable with the implant shelf-life. Our purpose was instead to study the wettability behavior on interval comparable with the implant storage life.

The second way takes advantage of two different processes that happen on the crystalline titania surface when it is exposed to a suitable UV irradiation ($\lambda < ca. 400$ nm, $E_g > 3.2$ eV): the photocatalytic oxidation process and the photoinduced

surface reorganization process (surface wettability conversion).[38,39] In other words, a UV treatment could re-establish the titania superhydrophilic behavior and, in the meantime, clean the surface (thanks to the photocatalytic removal of organic substances and the photoinduced surface reorganization).[38] Starting from the titania MOCVD coated samples stored in air for at least 20 days (and consequently with stable CA values, see Figure 5), it was found (Figure 6b) that 2 hours of UV treatment (irradiance: 58 W/m² at the samples level, UVC light, λ : 254 nm) were sufficient in order to completely restore the surface superhydrophilicity, with contact angle values close to zero for all the typologies of substrates. However, in the dark and in air, titania films return to a more hydrophobic state and it is due both to the organic recontamination of the surfaces and to the reversible change in titania surface structure under UV illumination (indeed the photogenerated -OH groups absorbed on the surface after UV irradiation are thermodynamically metastable). Finally, a slightly reduced loss of wettability appears when compared to the freshly deposited MOCVD TiO₂ coated surfaces (Figure 5) and it is likely due to the contribution of the photoinduced surface reorganization to the global wettability. As a conclusion, the Ti s+a_TiO₂ surfaces showed the best wettability behavior considering both the organic surface contamination and the storing in water.

3.2. Ion release tests

As a consequence of titanium corrosion, titanium ions are released in the volume surrounding the implant. It is revealed that Ti release affects the cellular differentiation processes, negatively influencing the whole process of healing and osseointegration.[5] Wachi et al.[40] proposed that Ti ions may induce inflammatory reaction and bone resorption around the implant. Moreover, Barao et al.[41] revealed that pathogenic bacteria are more easily accumulated on corroded surfaces and, therefore, inflammatory reactions around the implant could take place.

Additionally, in view of the long implant shelf life, dental implant failure could also be caused by adverse body reactions to titanium (such as Ti allergy). Even if some clinical studies on this topic have been carried out,[5] nowadays there is not enough data on the hypersensitivity to titanium and, consequently, more studies are necessary. Furthermore, rougher surfaces (i.e. with enhanced surface area) could be more prone to higher Ti release than smoother ones. Starting from these considerations, the aim of this study was to evaluate if an association between ion release and the implant surface area exists, and to understand if thin titania coatings could produce a beneficial contribute into this field.

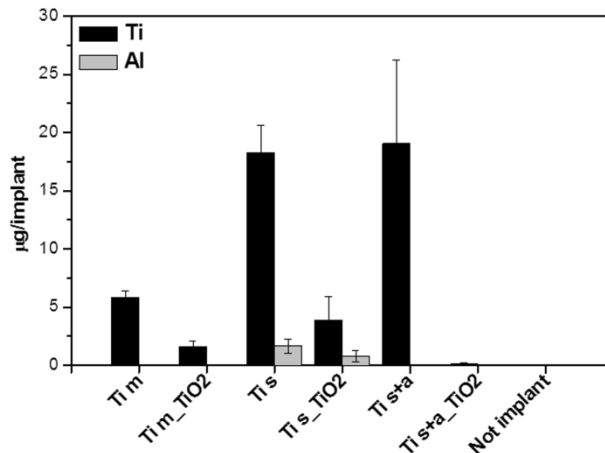


Figure 7. Amount of Ti and Al released (μg per implant) in lactic acid [LA] aqueous solution (pH=2.4) for uncoated or titania MOCVD coated implants. The implants had exactly the same geometrical size and weight.

Ti and Al ion releases (Figure 7) were evaluated *in-vitro* by after incubation in 1% lactic acid aqueous (LA) solution and in 0.1 mol/L phosphate-buffered saline (PBS) solution. According to Wennerberg et al.[12], lactic acid aqueous solution is a more severe environment for Ti and Al corrosion, for all the samples investigated (both uncoated and coated). On the other hand, no significant amounts of titanium and/or aluminum were released in PBS solution. Differing from Wennerberg et al.,[12] significant differences (p-value= 0.05) of ion release between machined surface and the rougher ones were detected. On bare substrates, the Ti release depends on roughness of the samples and therefore on real area exposed to LA solution: rougher surfaces seem to be associated with a higher ion release. Considering the effect of the titania coatings, it can be observed that the TiO₂ films prevent ion release for all the sample typologies, but Ti dissolution rose from machined to sandblasted surfaces and plummeted on the roughest surfaces (s+a). This could be explained considering synergistic effects. Firstly, the increasing of ion release due to the enhancement of the surface area, secondly the effectiveness of the titania as a protective layer. This second aspect showed its best effect in the 's+a' coated sample (the multi-

level superficial structure, joint with a perfectly cleaned surface due to the acid etching, increased the titania coating adhesion features with a probable better mechanical film to substrate interlocking), [42,43] while in the sandblasted sample the presence of alumina residues could negatively influence the first titania nucleation steps.

Finally, Al release was detected only in the sandblasted implants, confirming only in this sample the presence of Al_2O_3 residues from sandblasting process. Furthermore, as for titanium ion release, it can be observed that the TiO_2 coating did not totally prevent the Al release in LA. To sum up, the functionalization of the titanium surface with the titania layer can be a good strategy to reduce the ion release and consequently achieve a better osseointegrative capability.

3.3. Tribocorrosion and potentiodynamic polarization analyses

Open Circuit Potential (OCP) measurements consist in monitoring the potential difference between the sample under investigation (working electrode) and a reference electrode, both immersed in artificial saliva (AS) as an electrolytic solution. The electrochemical potential is a measure of the tendency to corrosion of the material under investigation: higher OCP values are related to nobler behavior of materials. [13] Different OCP values can be observed before sliding phase (Figure 8a) between uncoated and TiO_2 MOCVD coated samples, which demonstrated the beneficial increase of electrochemical nobility for coated surfaces in comparison to native passive films (i.e. thin and compact titania layers act as a more stable protective layer than the native passivation film). The uncoated samples showed low OCP values (i.e. -0.16 V, -0.10 V, and -0.03 V for Ti m, Ti s and Ti s+a, respectively), thus revealing a higher tendency to corrosion in AS, while the corresponding coated sample (with +0.04 V for Ti m- TiO_2 , +0.08 V for Ti s- TiO_2 , and +0.05 V for Ti s+a- TiO_2) exhibited nobler features. Hence, it is evident that MOCVD treatment could enhance the corrosion resistance of Ti surfaces in AS.

In a sliding dynamic contact, OCP describes the galvanic coupling evolution between the undamaged area (which develops a passive film, in the case of most biomaterials) and the corroded region, where the bare metal of substrate is exposed to the solution, due to the failure of the passive (or deposited) film during sliding. [44] For all samples, the potential values dropped to less noble values, as soon as the mechanical stress starts (onset of sliding), indicating the beginning of wear process with the partial/total destruction of the passive/deposited film. [2]

Among the uncoated substrates, Ti s demonstrated to be the noblest one, because of the presence of Al_2O_3 residuals from the sandblasting process, as it was observed in SEM/EDS and XRD characterizations. Ti s+a uncoated sample exhibited an irregular trend with two different phases, that could be ascribed to the initial presence and subsequent removal of the superficial acid etched layer. Finally, Ti m sample was the less noble surface.

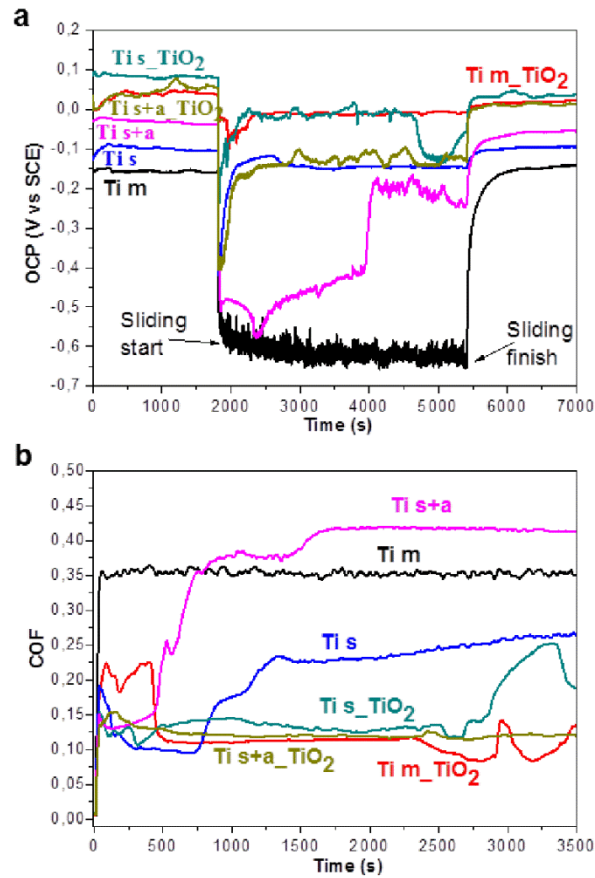


Figure 8. Open circuit potential (OCP) evolution for uncoated and MOCVD coated samples immersed in AS at 37°C before, during and after the sliding phase (a). Coefficient of friction (COF) during the sliding phase for uncoated and MOCVD coated samples immersed in AS at 37°C (b).

However, OCP values of coated samples are higher than those of corresponding uncoated ones; therefore TiO₂ films demonstrated to effectively protect the underlying Ti material from the direct contact with AS as long as it was in contact (it seems that the substrate surfaces were not exposed to the environment, or at least not in significant extension, and just a partial deterioration of the films occurred). Once the stress has been removed, a potential recovery towards more cathodic values was observed for all samples.[13] It is necessary to specify that the collected OCP values after sliding test represent a sum of different contributions given by both the wear track, where a damaged and/or missing protective film could be ascribed, and from the surrounding unperturbed area, where the deposited film remained untouched (that was the larger area), which supplied the highest contribution. Titania coatings on Ti m substrates appeared to possess the better coating behavior. Indeed, during the rubbing, OCP decreased only a few tenths of millivolts (from 0.04 V to -0.01 V), which could be associated to the wear of the topmost film layers, and increased again to its initial value when unloading.

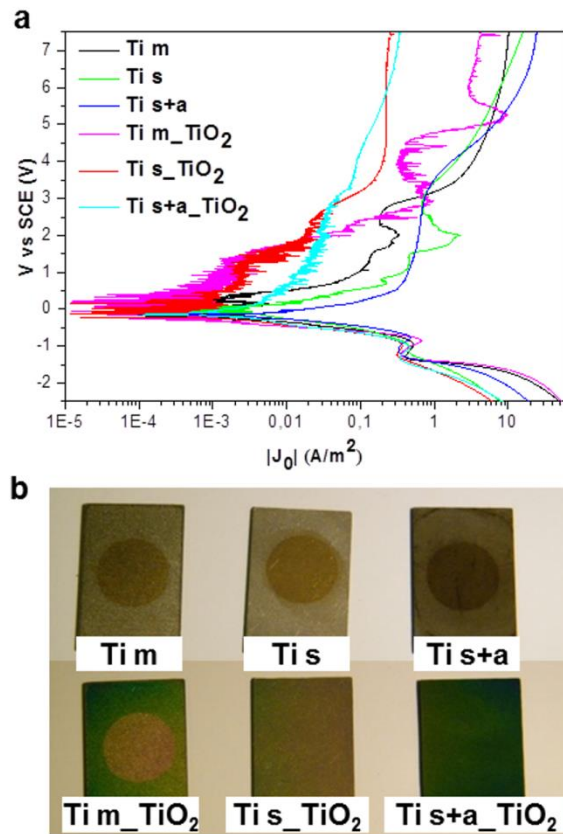


Figure 9. Potentiodynamic polarization curves of the uncoated and TiO₂-coated samples in AS at 37°C (a). Photos the sample surfaces after the potentiodynamic polarization experiments (b).

Sample	ΔE_{pass} (V)	$ j _{\text{pass}}$ (A/m ²)
Ti m	1.1÷2.8	0.2
Ti s	1÷3.25	0.6
Ti s+a	0.55÷3.2	0.55
Ti m_TiO ₂	2.1÷4.5	0.045
Ti s_TiO ₂	>1.8	0.22
Ti s+a_TiO ₂	>2.8	0.023

Table 1. ΔE_{pass} (region of passivity) and $|j|_{\text{pass}}$ (passivity current density) parameters obtained from potentiodynamic polarization curves of uncoated and MOCVD coated samples immersed in AS at 37°C.

In Figure 8b, the evolution of the coefficient of friction (COF) with the sliding time for uncoated and MOCVD coated Ti samples, is shown. Generally, COF values for coated Ti substrates are lower and their fluctuation are smoother than that of un-treated Ti samples, with a maximum gap of about 0.25 for the 'm' and 's+a' coated substrates. These differences in the COF values could be partially associated with the peculiar surface features of uncoated and coated samples[2], in particular the chemical nature and mechanical properties of the deposited coating, and also indicate that MOCVD coatings on cp-Ti have improved the anti-friction characteristics of the final material. Since the adhesion depends on the physical, chemical and mechanical properties of the coupled surfaces, the chemical relation between the TiO₂ and the counter body material is tribologically favorable in the case of MOCVD film in respect to the native oxide that spontaneously forms on Ti surface. Therefore deposited TiO₂ exhibited a lower COF reasonably ascribable to the chemical modification of surfaces, whereas physical and mechanical properties were the same for each type of sample surface (m, s, s+a).

For both s and s+a types, the COF exhibited an initial rapid increase due to the enlargement of contact surface as a result of wear effect on roughness ridges. The rise of surface available to couple to the counterpart generally increases the adhesive forces responsible for wear phenomena, thus enhancing COF values. The same was not observed in the corre-

sponding coated samples, indicating that the presence of a low-friction coupling was able to avoid or at least slow down the process of wear on roughness ridges. Moreover, in the case of the s+a finishing, the coating operated an effective and positive action during the overall tribological test, while s-type sample, although coated, reached a failure point with a sudden increase of COF after 2500 s. Also m-type finishing in the coated sample exhibited a good behavior and showed instability of COF at the same point as s-type sample. This demonstrates that TiO₂ coating represents a promising surface modification towards improved tribological properties of underlying material. More in detail, for Ti s_TiO₂ sample the COF value had a sudden increase exactly when the OCP curve showed a rapid reduction of the OCP value. For this sample a partial coating breakage was possible: after this event the COF value for the Ti s_TiO₂ sample becomes very similar to that of Ti s one.

Potentiodynamic polarization curves are shown in Figure 9, while ΔE_{pass} (region of passivity) and $|j|_{\text{pass}}$ (passivity current density) values are reported in Table 1. Potentiodynamic plots were obtained by scanning the applied voltage from -2.5 to 7.5 V vs SCE at a scanning rate of 2 mV/s, in artificial saliva thermostated at 37°C. J_0 was calculated considering also the Sdr values obtained from profilometry results. Thus, the actual exposed area was evaluated for each sample, taking into account the contribution of surface roughness. All the curves (Figure 9a) showed the typical shape of an active-passive behavior: all substrates demonstrate a passive region, which extends from OCP potential value to several volts, depending on the kind of sample.

The most interesting aspect was that coated samples exhibited lower j_{pass} and wider passive regions compared to the corresponding uncoated surfaces. Since the passivation action is due to the presence of TiO₂ (both native or MOCVD deposited) on the surfaces, these values clearly showed the improvement of electrochemical behavior for the coated samples. Moreover, it should be underlined that, even after that the potential was scanned to 7.5 V vs SCE, Ti s_TiO₂ and Ti s+a_TiO₂ samples did not corrode (there were no breakdown of the protective films, detectable from the absence of sharp growths of the current density in the anodic region). This finding could also be seen in Figure 9b, where the sample surfaces (both uncoated and coated), after the potentiodynamic test, are shown. It can be clearly observed that on Ti s_TiO₂ and Ti s+a_TiO₂ samples, the presence of surface damage, after the potentiodynamic experiment, was not evident.

3.4. Nanoindentation investigations

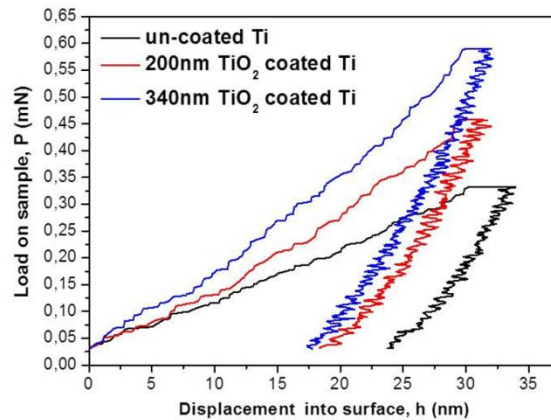


Figure 10. Average nanoindentation load-displacement curve for uncoated Ti substrate and MOCVD coated Ti substrates (200 nm and 335 nm thick).

Taking into account the requisites for an optimal indentation test (i.e. no influence on the mechanical properties of the film due to substrate if the indentation depth is smaller than 1/10 of the overall film thickness)[45] and the drawback due to the too high roughness of the here evaluated samples, comparable with the thickness of the titania MOCVD film,[4] nanoindentation tests cannot be directly performed on the “m”, “s” and “s+a” samples. Nevertheless, it appears to be of high relevance the investigation of the superficial Hardness and the Elastic modulus variation when titanium is MOCVD coated with TiO₂. Because of this reason, *ad-hoc* sample has been prepared by smoothing the Ti substrate to a 60-80 nm of residual R_a, and coating it with a thicker TiO₂ layer (i.e. 335 nm). Moreover, for the sake of completeness, a TiO₂ coating of 200 nm was also obtained and investigated, thus providing more realistic Hardness and the Elastic modulus compared to the TiO₂ layer here deposited on the Ti m, Ti s and Ti s+a samples.

The nanoindentation tests were then performed on the smoothed Ti substrates and on the 200 and 335 nm TiO₂ coated samples; the uncoated smoothed substrate was used as reference. Figure 10 shows the typical load-displacement curves

for Ti substrate and TiO₂ thin films deposited on smooth cp-Ti, while Table 2 displays the mean hardness (H) and elastic modulus (E).

Substrate	H(GPa)	E(GPa)	Max penetration depth (nm)
Ti	6.63±0.63	197±21	34±1
Ti_TiO ₂ (200nm)	9.97±2.53	197±40	32±1
Ti_TiO ₂ (335 nm)	16.25±3.34	264±42	31±1

Table 2. Mean value of hardness (H) and Elastic Modulus (E) for uncoated Ti substrate and MOCVD coated Ti substrates (200 nm and 335 nm).

Clearly, the pristine Ti had a very low hardness, while TiO₂ films increased the Ti mechanical properties drastically, as indicated by the higher indentation maximum load achieved for the same displacement. In literature, the hardness of titania thin film varies from 2 to 13 GPa[46] as function of the thin film deposition method and/or the crystalline phase.[47] Comparing the H values of bare substrates with the MOCVD treated ones (Table 2), higher H values (at 0.05 level of significance) can be observed for the coated samples than that of bulk metallic substrates. This is reasonable because generally oxide materials are harder than metallic ones, due to their covalent chemical nature. Finally, lower H value was detected in Ti_TiO₂ (200 nm) samples in comparison with Ti_TiO₂ (335 nm). As it was mentioned before, in the case of thin films and for penetration depth higher than 10% of film thickness, the mechanical response is a combination of the contribution from the coating and the substrate. As can be observed in Table 2, the mean penetration depth for the Ti_TiO₂ (200 nm) samples was higher than a tenth of the film thickness (32 nm > ~20 nm), consequently the detected values were (at least partially) influenced by the underlying Ti substrate.

The Elastic modulus (E) of the titania coatings on the Ti substrates appeared very similar to the values reported in the literature for anatase TiO₂. [4,48,49] There is no statistical difference (at 0.05 level of significance) in Elastic modulus of 200nm_TiO₂ coated Ti and uncoated Ti substrate, providing good conditions for mechanical deformation of the composite material. Finally, the average values of H and E for the bulk titanium were higher than those reported in literature.[49] To sum up, the mechanical properties of the bulk titanium were also improved with the deposition of TiO₂ thin film and the observed outcomes can suggest interesting positive effects on the actual investigated sample (Ti m, Ti s, Ti s+a).

CONCLUSION

Modifying dental implant surface morphology and composition can be a key issue for improving osseointegration. This paper is focused on the development of a new typology of titanium surfaces, where the main goal is the improvement of the surface characteristics in order to achieve a better osseointegration. In this paper, LP-MOCVD technique was employed to deposit conformal crystalline TiO₂ layers on Ti substrates with the aim of improving the titanium superficial properties. From SEM and profilometer analyses, it was shown that MOCVD is a reliable technique for coating Ti substrates, with an optimal conformal coverage, and the TiO₂ films perfectly match the profile of the substrate below. X-Ray Diffraction analyses revealed that the TiO₂ layers grow as anatase, while only in the sandblasted substrates the rutile phase was also detected. Wettability studies suggested improved hydrophilic behavior for the coated surfaces compared to bare Ti, thus allowing a better degree of contact with the physiological environment. The freshly coated titania surfaces showed superhydrophilic features, but TiO₂ coated samples decreased their wettability when stored in air due to hydrocarbon contamination. In order to maintain the high energy surfaces two industrial-scalable strategies were set-up: i) storing the products under water or ii) the restoration of the superhydrophilicity by UV treatment. The sample storing in water appears simple, cost-effective and allows the preservation of the products with high hydrophilic behavior for several months, but it did not completely guarantee the superhydrophilic characteristic, especially over long period of conservation, comparable with sterility shelf life. The UV treatment, although it requires an UV light source, appears to be of high relevance because it can be seen as an “on-demand” restoration technique, i.e. to be used just before the use of the product (before the implantation). Ion (Ti and Al) release studies showed that the functionalization of the titanium surface with the titania layer was a good strategy to reduce the ion release and the roughest coated surfaces (Ti s+a_TiO₂) showed the low ion release. Tribocorrosion experiments indicated that TiO₂ films were able to (almost totally) effectively protect the Ti surfaces from the direct contact with artificial saliva; better COF values were also detected for the coated surfaces in comparison with the uncoated ones. Potentiodynamic polarization experiments showed that TiO₂ thin film could im-

prove the electrochemical behavior on titanium substrates. Finally comparing the hardness (H) values of the bare Ti with those of the coated ones, higher H values were observed for the coated samples: this means that the mechanical properties of the titanium bulk were improved with the functionalization.

As a conclusion, sandblasted/acid etched LP-MOCVD TiO₂ coated Ti substrates generally showed the best performance of functional properties; moreover, considering that they had a clean surface (no presence of residues) and a high surface area enable to favor a good mechanical interlocking with bone, the 200 nm titania coated s+a surfaces seem to be the best materials for dental implant applications.

AUTHOR INFORMATION

Author Contributions

F. V., A. G. and N. E. H. contributed to the conception and design of the study.

F. V. performed the samples preparation, the wettability and roughness analyses. A. G. realized s+a surfaces. S. B. did SEM –EDS analyses. N.B. performed ICP-AES experiments. V. Z. carried out tribocorrosion, potentiodynamic polarization and nanoindentation experiments. N. E. H carried out structural characterization.

The manuscript was written by F. V. All authors discussed, revised, and approved the final manuscript.

Funding Sources

This work was supported by ‘RT Unipersonale srl’, now ‘Mech & Human’.

ACKNOWLEDGMENTS

The authors acknowledge ‘RT Unipersonale srl’, now ‘Mech & Human’, in relation to Francesca Visentin’s PhD grant and for the substrates supply. The authors acknowledge Mr. Renzo Tagliaro for the helpful discussions.

REFERENCES

- [1] M. Zuldesmi, A. Waki, K. Kuroda, M. Okido, Hydrothermal treatment of titanium alloys for the enhancement of osteoconductivity, *Materials Science and Engineering C*. 49 (2015) 430–435. doi:10.1016/j.msec.2015.01.031.
- [2] S.A. Alves, R. Bayón, A. Igartua, V.S. De Viteri, L.A. Rocha, Tribocorrosion behaviour of anodic titanium oxide films produced by plasma electrolytic oxidation for dental implants, *Lubrication Science*. 26 (2014) 500–513. doi:10.1002/lis.1234.
- [3] Y.T. Sul, The significance of the surface properties of oxidized titanium to the bone response: Special emphasis on potential biochemical bonding of oxidized titanium implant, *Biomaterials*. 24 (2003) 3893–3907. doi:10.1016/S0142-9612(03)00261-8.
- [4] M. Lorenzetti, E. Pellicer, J. Sort, M.D. Baró, J. Kovač, S. Novak, S. Kobe, Improvement to the corrosion resistance of Ti-based implants using hydrothermally synthesized nanostructured anatase coatings, *Materials*. 7 (2014) 180–194. doi:10.3390/ma7010180.
- [5] Z. Stanec, J. Halambek, K. Maldini, M. Balog, P. Križik, Z. Schauerperl, A. Catic, Titanium Ions Release from an Innovative Titanium-Magnesium Composite: an in Vitro Study, *Acta Stomatologica Croatica*. 50 (2016) 40–48. doi:10.15644/asc50/1/6.
- [6] L.T. De Jonge, S.C.G. Leeuwenburgh, J.G.C. Wolke, J.A. Jansen, Organic-inorganic surface modifications for titanium implant surfaces, *Pharmaceutical Research*. 25 (2008) 2357–2369. doi:10.1007/s11095-008-9617-0.
- [7] D. Duraccio, F. Mussano, M.G. Faga, Biomaterials for dental implants: current and future trends, *Journal of Materials Science*. 50 (2015) 4779–4812. doi:10.1007/s10853-015-9056-3.
- [8] A. Jemat, M.J. Ghazali, M. Razali, Y. Otsuka, Surface modifications and their effects on titanium dental implants, *BioMed Research International*. (2015) 791725. doi:10.1155/2015/791725.
- [9] M. Yamamura, K.; Miura, T.; Kou, I; Muramatsu, T.; Furusawa, M.; Yoshinari, Influence of various superhydrophilic treatments of titanium on the initial attachment, proliferation, and differentiation of osteoblast-like cells, *Dental Materials Journal*. 34 (2015) 120–127. doi:10.4012/dmj.2014-076.
- [10] K. Kubo, N. Tsukimura, F. Iwasa, T. Ueno, L. Saruwatari, H. Aita, W.A. Chiou, T. Ogawa, Cellular behavior on TiO₂ nanonodular structures in a micro-to-nanoscale hierarchy model, *Biomaterials*. 30 (2009) 5319–5329. doi:10.1016/j.biomaterials.2009.06.021.
- [11] D.L. Cochran, R.K. Schenk, A. Lussi, F.L. Higginbottom, D. Buser, Bone response to unloaded and loaded titanium implants with a sandblasted and acid-etched surface: A histometric study in the canine mandible, *Journal of Biomedical Materials Research*. 40 (1998) 1–11. doi:10.1002/(SICI)1097-4636(199804)40:1<1::AID-JBM1>3.0.CO;2-Q.
- [12] A. Wennerberg, A. Ide-Ektessabi, S. Hatkamata, T. Sawase, C. Johansson, T. Albrektsson, A. Martinelli, U.

- Södervall, H. Odellius, Titanium release from implants prepared with different surface roughness: An in vitro and in vivo study, *Clinical Oral Implants Research*. 15 (2004) 505–512. doi:10.1111/j.1600-0501.2004.01053.x.
- [13] I. da S.V. Marques, M.F. Alfaro, M.T. Saito, N.C. da Cruz, C. Takoudis, R. Landers, M.F. Mesquita, F.H. Nociti Junior, M.T. Mathew, C. Sukotjo, V.A.R. Barão, Biomimetic coatings enhance tribocorrosion behavior and cell responses of commercially pure titanium surfaces, *Biointerphases*. 11 (2016) 031008–031014. doi:10.1116/1.4960654.
- [14] A. Radtke, A. Topolski, T. Jędrzejewski, W. Kozak, B. Sadowska, M. Więckowska-Szakiel, P. Piszczek, Bioactivity Studies on Titania Coatings and the Estimation of Their Usefulness in the Modification of Implant Surfaces, *Nanomaterials*. 7 (2017) 90. doi:10.3390/nano7040090.
- [15] S. Popescu, I. Demetrescu, C. Sarantopoulos, A.N. Gleizes, D. Iordachescu, The biocompatibility of titanium in a buffer solution: Compared effects of a thin film of TiO₂ deposited by MOCVD and of collagen deposited from a gel, *Journal of Materials Science: Materials in Medicine*. 18 (2007) 2075–2083. doi:10.1007/s10856-007-3133-3.
- [16] Z. Karaji, B. Houshmand, S. Faghihi, Surface Modification of Porous Titanium Granules for Improving Bioactivity, *The International Journal of Oral & Maxillofacial Implants*. 31 (2016) 1274–1280. doi:10.11607/jomi.5246.
- [17] A. Cimpean, S. Popescu, C.M. Ciofrangeanu, A.N. Gleizes, Effects of LP-MOCVD prepared TiO₂ thin films on the in vitro behavior of gingival fibroblasts, *Materials Chemistry and Physics*. 125 (2011) 485–492. doi:10.1016/j.matchemphys.2010.10.028.
- [18] M. Baryshnikova, L. Filatov, M. Mishin, A. Kondrateva, S. Alexandrov, Formation of hydroxylapatite on CVD deposited titania layers, *Physica Status Solidi C*. 12 (2015) 918–922. doi:10.1002/pssc.201510015.
- [19] P.C. Rath, L. Besra, B.P. Singh, S. Bhattacharjee, Titania/hydroxyapatite bi-layer coating on Ti metal by electrophoretic deposition: Characterization and corrosion studies, *Ceramics International*. 38 (2012) 3209–3216. doi:10.1016/j.ceramint.2011.12.026.
- [20] H.W. Kim, Y.H. Koh, L.H. Li, S. Lee, H.E. Kim, Hydroxyapatite coating on titanium substrate with titania buffer layer processed by sol-gel method, *Biomaterials*. 25 (2004) 2533–2538. doi:10.1016/j.biomaterials.2003.09.041.
- [21] S. Bauer, P. Schmuki, K. von der Mark, J. Park, Engineering biocompatible implant surfaces: Part I: Materials and surfaces, *Progress in Materials Science*. 58 (2013) 261–326. doi:10.1016/j.pmatsci.2012.09.001.
- [22] S. Popescu, I. Demetrescu, V. Mitran, A.N. Gleizes, MOCVD-fabricated TiO₂ thin films: Influence of growth conditions on fibroblast cells culture, *Molecular Crystals and Liquid Crystals*. 483 (2008) 266–274. doi:10.1080/15421400801914301.
- [23] L. Tagliaro, R.; Visentin, F.; El Habra, N.; Armelao, Coating titanium-based substrate for e.g. biomedical applications by vapor deposition of compact intermediate layer based on crystalline titania and spray pyrolysis of homogeneous, discontinuous layer of phosphorus and calcium derivatives, Patent application WO2018096483-A1, n.d.
- [24] L. Lutterotti, MAUD—Materials Analysis Using Diffraction., (n.d.). <http://maud.radiographema.com/> (accessed November 1, 2018).
- [25] H. Li, J.J. Vlassak, Determining the elastic modulus and hardness of an ultra-thin film on a substrate using nanoindentation, *Journal of Materials Research*. 24 (2009) 1114–1126. doi:10.1557/jmr.2009.0144.
- [26] W.C. Oliver, G.M. Pharr, An improved technique for determining hardness and elastic modulus using load and displacement sensing indentation experiments, *Journal of Materials Research*. 7 (1992) 1564–1583. doi:10.1557/JMR.1992.1564.
- [27] C. Sarantopoulos, E. Puzenat, C. Guillard, J.M. Herrmann, A.N. Gleizes, F. Maury, Microfibrous TiO₂ supported photocatalysts prepared by metal-organic chemical vapor infiltration for indoor air and waste water purification, *Applied Catalysis B: Environmental*. 91 (2009) 225–233. doi:10.1016/j.apcatb.2009.05.029.
- [28] X. Lin, L. Zhou, S. Li, H. Lu, X. Ding, Behavior of acid etching on titanium: Topography, hydrophilicity and hydrogen concentration, *Biomedical Materials (Bristol)*. 9 (2014) 015002. doi:10.1088/1748-6041/9/1/015002.
- [29] H. Chatbi, M. Vergnat, G. Marchal, Thermal stability of titanium hydride thin films, *Applied Physics Letters*. 64 (1994) 1210–1211. doi:10.1063/1.111950.
- [30] D. Buser, N. Brogini, M. Wieland, R.K. Schenk, A.J. Denzer, D.L. Cochran, B. Hoffmann, A. Lussi, S.G. Steinemann, Enhanced bone apposition to a chemically modified SLA titanium surface, *Journal of Dental Research*. 83 (2004) 529–533. doi:10.1177/154405910408300704.
- [31] G. Zhao, Z. Schwartz, M. Wieland, F. Rupp, J. Geis-Gerstorfer, D.L. Cochran, B.D. Boyan, High surface energy enhances cell response to titanium substrate microstructure, *Journal of Biomedical Materials Research - Part A*. 74 (2005) 49–58. doi:10.1002/jbm.a.30320.
- [32] N.P. Lang, G.E. Salvi, G. Huynh-Ba, S. Ivanovski, N. Donos, D.D. Bosshardt, Early osseointegration to hydrophilic and hydrophobic implant surfaces in humans, *Clinical Oral Implants Research*. 22 (2011) 349–356. doi:10.1111/j.1600-0501.2011.02172.x.
- [33] F. Rupp, L. Scheideler, D. Rehbein, D. Axmann, J. Geis-Gerstorfer, Roughness induced dynamic changes of wettability of acid etched titanium implant modifications, *Biomaterials*. 25 (2004) 1429–1438. doi:10.1016/j.biomaterials.2003.08.015.
- [34] H. Lu, L. Zhou, L. Wan, S. Li, M. Rong, Z. Guo, Effects of storage methods on time-related changes of titanium

surface properties and cellular response, *Biomedical Materials (Bristol)*. 7 (2012) 055002. doi:10.1088/1748-6041/7/5/055002.

- [35] M.D. Sartoretto, S.C.; Alves, A.T.N.N.; Resende, R.F.B.; Calasans-Maia, J.; Granjeiro, J.M.; Calasans-Maia, Early osseointegration driven by the surface chemistry and wettability of dental implants, *Journal of Applied Oral Science*. 23 (2015) 279–287. doi:10.1590/1678-775720140483.
- [36] D. Yamamoto, K. Ariei, K. Kuroda, R. Ichino, M. Okido, A. Seki, Osteoconductivity of Superhydrophilic Anodized TiO₂ Coatings on Ti Treated with Hydrothermal Processes, *Journal of Biomaterials and Nanobiotechnology*. 4 (2013) 45–52. doi:10.4236/jbnb.2013.41007.
- [37] S. Li, J. Ni, X. Liu, X. Zhang, S. Yin, M. Rong, Z. Guo, L. Zhou, Surface characteristics and biocompatibility of sandblasted and acid-etched titanium surface modified by ultraviolet irradiation: An in vitro study, *Journal of Biomedical Materials Research - Part B Applied Biomaterials*. 100 B (2012) 1587–1598. doi:10.1002/jbm.b.32727.
- [38] A. Mills, M. Crow, A study of factors that change the wettability of titania films, *International Journal of Photoenergy*. 2008 (2008) 470670. doi:10.1155/2008/470670.
- [39] M. Lorenzetti, D. Biglino, S. Novak, S. Kobe, Photoinduced properties of nanocrystalline TiO₂-anatase coating on Ti-based bone implants, *Materials Science and Engineering C*. 37 (2014) 390–398. doi:10.1016/j.msec.2014.01.029.
- [40] T. Wachi, T. Shuto, Y. Shinohara, Y. Matono, S. Makihira, Release of titanium ions from an implant surface and their effect on cytokine production related to alveolar bone resorption, *Toxicology*. 327 (2015) 1–9. doi:10.1016/j.tox.2014.10.016.
- [41] V.A.R. Barão, M.T. Mathew, W.G. Assunção, J.C.C. Yuan, M.A. Wimmer, C. Sukotjo, Stability of cp-Ti and Ti-6Al-4V alloy for dental implants as a function of saliva pH - an electrochemical study, *Clinical Oral Implants Research*. 23 (2012) 1055–1062. doi:10.1111/j.1600-0501.2011.02265.x.
- [42] G. Wahl, Protective Coatings, in: Hitchman, M.L., Jensen, K.F. (Ed.), *Chemical Vapor Deposition, Principle and Applications*, Academic Press: San Diego, CA, 1993: pp. 591–662.
- [43] M. Ohring, *Materials Science of Thin Films*, second, Academic Press: San Diego, CA, 2002. doi:10.1016/B978-0-12-524975-1.50018-5.
- [44] L.A. Cruz, H. V.; Souza, J. C. M.; Henriques, M.; Rocha, No Title, in: *Biomedical Tribology*, Nova Science Publishers: Hauppauge, NY, 2011: pp. 1–33.
- [45] A.C. Fischer-Cripps, *Nanoindentation*, Springer: New York, 2004.
- [46] D. Wojcieszak, M. Mazur, J. Indyka, A. Jurkowska, M. Kalisz, P. Domanowski, D. Kaczmarek, J. Domaradzki, Mechanical and structural properties of titanium dioxide deposited by innovative magnetron sputtering process, *Materials Science- Poland*. 33 (2015) 660–668. doi:10.1515/msp-2015-0084.
- [47] A. Bendavida, P.J. Martina, H. Takikawa, Deposition and modification of titanium dioxide thin films by filtered arc deposition., *Thin Solid Films*. 360 (2000) 241–249.
- [48] W.J. Yin, S. Chen, J.H. Yang, X.G. Gong, Y. Yan, S.H. Wei, Effective band gap narrowing of anatase TiO₂ by strain along a soft crystal direction, *Applied Physics Letters*. 96 (2010) 221901. doi:10.1063/1.3430005.
- [49] P. Soares, A. Mikowski, C.M. Lepienski, E. Santos, G.A. Soares, V. Swinka Filho, N.K. Kuromoto, Hardness and elastic modulus of TiO₂ anodic films measured by instrumented indentation, *Journal of Biomedical Materials Research - Part B Applied Biomaterials*. 84B (2008) 524–530. doi:10.1002/jbm.b.30900.

Graphical abstract

